FINAL REPORT TO THE STATE OF CALIFORNIA AIR RESOURCES BOARD

CONTRACT ARB-1116

FATE AND DISTRIBUTION OF INHALED NITROGEN DIOXIDE IN THE NON-HUMAN PRIMATE

by

Elliot Goldstein, M.D., Neal F. Peek, Ph.D., and Norris J. Parks, Ph.D.

University of California, Davis

Davis, California 95616

Abstract

The intra and extrapulmonary distribution of inspired nitrogen dioxide was studied by exposing Rhesus Monkeys to air mixtures containing 0.3 to 0.9 ppm nitrogen-13 (half period = 10 min), nitrogen dioxide ($^{13}NO_2$). The $^{13}NO_2$ was synthesized by the ^{16}O $(p,\alpha)^{13}$ N nuclear reaction. Pulmonary and blood concentrations of $^{13}NO_2$ were continuously detected by external monitoring of the annihilation radiation consequent to positron emissions (511 KeV) from disintegrating ^{13}N atoms. Control studies were performed in an identical manner with xenon-125 (^{125}Xe).

According to the results which were obtained approximately fifty percent of the inspired nitrogen dioxide was removed by the primate during normal respiration. The gas distributed itself throughout the lungs with slightly higher concentrations occurring in the central pulmonary regions than in the more peripheral areas. Once absorbed by the lungs, nitrogen dioxide or a chemical derivative remained for prolonged periods following cessation of exposure. The blood concentration of nitrogen dioxide or a chemical derivative increased in parallel with that for the lungs.

These data indicate that the air pollutant, nitrogen dioxide, interacts extensively with pulmonary tissues and that the pollutant itself or chemically related products accumulate within the lungs and blood.

This report was submitted in fulfillment of Air Resources Board Contract 1116 by The Regents of the University of California under the partial sponsorship of the California Air Resources Board. Work was completed as of 30 August, 1974.

Table of Contents

Figures

Acknowledgement

The authors wish to express appreciation for scientific and technical assistance to Dr. E.P. Steffey, B. Tarkington, T. Duval, of the Veterinary School of Medicine; H. Hines and J. Schwind of Crocker Nuclear Laboratory, Professor J.W. Root of Nuclear Chemistry, and Mr. S. Leung of the Air Resources Board. This report is dedicated to the memory of Mr. Dale H. Hutchison, whose interest and enthusiasm in this project were major factors in its accomplishment.

Conclusions:

1. Nitrogen -13 dioxide ($^{13}NO_2$) can be synthesized and produced in sufficient quantities for biological experimentation by bombarding a high purity oxygen target with 15 MeV protons and then cryogenically separating the $^{13}NO_2$ from other primary products such as 13-N, and 13N-NO.

2. Exposure of non-human primates to near ambient concentrations of $^{13}NO_2$ (0.3 - 0.9 ppm), results in the intrapulmonary absorption of approximately 50% of the inspired pollutant.

3. Maximum absorption of the pollutant occurs within the central pulmonary regions as opposed to the more peripheral alveolar areas.

4. The extent of absorption increased in accordance with the concentration and duration of pollutant exposure.

5. Pulmonary retention of the nitrogen dioxide or a chemical derivative was 100% during the wash-out period following cessation of exposure. As such, pulmonary removal mechanisms were non-existant under these near ambient exposure conditions.

6. Nitrogen dioxide or a chemical derivative entered the blood with ease. The pollutant concentration within the blood paralleled the pulmonary concentration.

7. These experiments indicate that in non-human primates the inspiration of near ambient concentrations of nitrogen dioxide results in the chemical interaction of approximately 50% of the pollutant with pulmonary tissues. Because this effect increases with degree and duration of exposure, it is likely to result in biological consequences.

Recommendations:

These experiments can be considered a self-encompassing project. They were undertaken to determine 1) if the inspiration of near ambient concentrations of nitrogen dioxide resulted in specific areas of interaction of pollutant and pulmonary tissue and 2) if a build-up in concentration of pollutant occurred within the lungs or if a steady-state of interaction resulted which would protect the lungs from increasingly severe pollutant exposure. The data clearly indicate that nitrogen dioxide reacts throughout the lungs with some increase in interaction in the central pulmonary regions. Because the removal mechanisms for the gas are virtually non-existant, pulmonary damage, if it should occur, would tend to be progressive even though the exposure remained at a relatively low level. Such an explanation can account for the heretofore disparate findings that brief exposures to low levels of nitrogen dioxide do not cause pulmonary toxicity, whereas prolonged exposures to the same concentrations of nitrogen dioxide are associated with pathophysiological consequences.

Future experiments of a similar nature with other gaseous pollutants (sulfur dioxide, ozone, peroxyacetyl nitrate etc.) or combinations of these pollutants with particulates would seem appropriate. Such experiments would delineate whether these agents act at specific sites within the lung and if this interaction increases with the duration of exposure. In particular, the possibility that inspired sulfur dioxide by itself or together with commonly occurring particulates interacts in specific pulmonary regions to cause progressively more severe tissue injury is critical for an understanding of the toxic effects of these agents. This information would also delineate the kinds of biological tests which would be the most sensitive indicators of pollutant induced damage. The identification of target areas of pollutant toxicity would be helpful in estimating the effect of pollutant exposure in individuals with underlying diseases.

As an example, patients with damage to their small bronchi due to chronic bronchitis might be at particular risk if the inspiration of sulfur dioxide and particulates of one to three micra results in the preferential deposition of the pollutant on the already damaged bronchial sites.

Disclaimer:

The statements and conclusions in this report are those of the contractor and not necessarily those of the California Air Resources Board. The mention of commercial products, their source or their use in connection with material reported herein is not to be construed as either an actual or implied endorsement of such products.

Introduction:

The intra and extrapulmonary distribution of an air pollutant is important in determining its biological toxicity. Pollutants such as sulfur dioxide that interact chemically within the nasopharynx and upper airways affect these regions primarily. [1-4] In contrast carbon monoxide penetrates the alveolar-blood barrier to cause extrapulmonary rather than intrapulmonary abnormalities. [1,5] Similar information regarding the interaction of nitrogen dioxide with tissues of the upper airways, alveoli and blood would be useful in predicting the likelihood of damage to these tissues.

The few studies of the fate of nitrogen dioxide indicate that a high percentage of the inspired gas is absorbed and that the reaction probably occurs within the distal pulmonary regions. [6-8] Von Nieding and co-workers showed that volunteers who inhale 0.94 mg/m^3 (0.5 ppm) to 9.4 mg/m^3 (5.0 ppm) of nitrogen dioxide retain 80 to 90 per cent of the pollutant.[6] Additional experiments with dogs and rabbits and with model airway systems which simulate the interaction of nitrogen dioxide and pulmonary tissues show most of the pollutant reaching the alveolar areas. [7,8]

The present investigations were designed to quantify the extent of reaction of nitrogen dioxide with individual pulmonary regions and with blood in non-human primates during and following exposure to 1.7 mg/m^3 (0.9 ppm) or less of the pollutant. Radioisotopically labeled Nitrogen-13 dioxide ($^{13}NO_2$) was synthesized in an isochronous cyclotron by a series of radionuclear reactions (9). The intrapulmonary location and concentration of the inspired $^{13}NO_2$ was continuously detected by external monitoring of the annihilation radiation consequent to positron emissions from disintegrating ^{13}N atoms. The ^{13}N concentration of the arterial blood was also measured at intervals and these values were correlated with those from the lung. The results of these experiments are documented in this report.

Materials and Methods

Animals. Adult female Rhesus monkeys weighing approximately 5 kg were obtained from the California Primate Research Center, University of California at Davis. The animals had been in good health for at least one year prior to the experiment.

Production of Radioactive $^{13}NO_2$. The radionuclear procedures for the synthesis and measurement of $^{13}NO_2$ have been published.[9] Briefly, oxygen gas at 15 atmospheres of pressure is circulated through a 15 MeV proton beam produced by the Crocker Nuclear Laboratory 76 inch

isochronous cyclotron. Radioactive ^{13}N atoms ($t_{1/2}$ = 10 min.) were produced by the $^{16}O(p,\alpha)^{13}N$ nuclear reaction. These atoms reacted with oxygen target molecules, radiation produced chemical species, and trace (< 20 ppm N_2) impurities to form $^{13}NO_2$, ^{13}N-NO, and ^{13}N-N. The effluent of the gas target was passed through a stainless steel cryogenic trap (-45°C) which permitted the NO_2/N_2O_4 fraction (fp = -9.3°C), to be separated from N_2 (bp = -196°C), N_2O fp = -88°C) and O_2 (bp = -183°C) After collection of 1-2 mCi's of activity, the trap was evacuated to 1 torr or less under low temperature conditions in order to remove remaining gaseous material. The trap contents, $^{13}NO_2$ and carrier NO_2 which was generated in situ by radiolysis of the trace nitrogen impurities, were reformed into the gas phase by warming and flushed into the spirometer reservoir with extremely dry air (Matheson "Zero Gas"). Because the concentrations of radiolytically produced NO_2 could not be accurately predicted, additional NO_2 at concentrations of up to (0.6 ppm) were added in some experiments. Ten liter (STP) aliquots of the experimental breathing mixture containing 0.3-0.9 ppm NO_2 labeled with 0.5-1.5 mCi of ^{13}N activity were prepared in this manner. Half-life determinations were made on all gas mixtures to insure the absence of radionuclides other than ^{13}N.

Production of ^{125}Xenon. Xenon-125, a non-reactive gas suitable for high resolution lung imaging was synthesized by bombarding a NaI target with 37 MeV protons to produce the ^{127}I (p,3n)^{125}Xe nuclear reaction. Cryogenic methods similar to the ones described for $^{13}NO_2$ were used to separate the ^{125}Xe from contaminating materials.[10]

Detection of radioactivity in Air and Blood. The radioactivity of 10 ml samples of inspired and expired air and 2.5 ml samples of heparinized blood was measured with a 2" by 2" NaI (Tℓ) detector. Background radiation was reduced to near zero by surrounding the detector with two inches of lead shielding. A single channel analyser with its window centered about the 511 KeV line received the amplified signal from the detector. The radioactivity of the samples was counted for 100 seconds. All values were converted to time 0 to correct for radioisotopic decay.

Dynamic Studies of Pulmonary Radioactivity. The distribution of radioactive $^{13}NO_2$ and ^{125}Xe within the upper abdomen and thorax of the primate was measured continuously with a Nuclear Data Selekironic Anger camera. The spatial resolution of the radioisotopic disintegration products was optimized with a high energy (550 KeV) parallel hole collimator. The camera was interfaced to a Digital Corporation PDP 15/40 computer so that its information could be accumulated and sequentially stored for each 10 second time period in 64 by 64 arrays on a magnetic tape. Scintiphotos were also obtained at minute intervals.

Analysis of Radiation Data. Quantitation of radioactivity within the lungs as a function of time was performed by summing the array points corresponding to the lung and subtracting an equal sized area of background. Pulmonary boundaries were clearly delineated in the experiments with ^{125}Xe The pulmonary borders were less distinct in the experiments with $^{13}NO_2$ due to diminished resolution of the camera for this higher energy radioisotope. This difficulty was compensated for by seating the primate in a restraining chair at a fixed distance from the Anger camera so that the same geometrical relationships applied for all radioisotopic measurements. The distinct pulmonary boundaries found with ^{125}Xe were superimposed onto the radioactivity records for $^{13}NO_2$.

Chemical Measurements. Nitrogen dioxide concentrations were determined by the Saltzman method. (11) One liter samples of air were drawn through two fritted nitrogen dioxide bubblers connected in series at a flow rate of 0.4 liter per minute. Each bubbler contained 10 ml of Saltzman reagent. After allowing 15 minutes for complete color development in the reagent, the samples were measured in a spectrophotometer set at 550 nm.

Physiological Measurements. The volume of inspired radioactive gas was measured with a Wright spirometer. Respiratory rates were recorded visually.

Operational and Evaluation Phase. Figure 1 is a schematic diagram of the experimental system. The radioactively labeled $^{13}NO_2$ was transferred at atmospheric pressure from the pressurized cylinder to the mylar reservoir by means of a needle valve. During inspiration the gas was drawn from the reservoir through a one meter stainless steel tube (15.8 mm in diameter), through a Wright spirometer and into a face mask containing a mouthpiece with a two-way valve. The volume of gas was measured as it passed through the Wright spirometer. Exhaled gas exited through similarly sized steel tubing into a second mylar reservoir. Samples of inspired and expired gas were removed for radioisotopic and chemical analysis via two small 6 mm in diameter stainless steel sampling ports which were welded into each one meter tube. The Anger camera was positioned behind the primate. Lead shielding surrounded the mylar reservoirs and the camera.

The experimental procedure consisted of anesthetizing the primate with 10 mg/kg of Ketamine, inserting a femoral catheter connected to a heparin source, and then placing the animal in the restraining chair where he was allowed to adjust to the face mask for 15 to 30 minutes. Attachment of the face mask to the inhalation and exhalation parts of the experimental system occurred as soon as the mylar reservoir was filled with $^{13}NO_2$ (time 0). Collection of 10 ml and 1.0 liter aliquots of inspired gas for determination of radioisotopic and chemical concentration of $^{13}NO_2$ began 30 or more seconds later. Thereafter, alternating

10 ml samples of expired and inspired gas were removed for radioactivity determinations. In two experiments an additional 1.0 liter specimen of expired gas was obtained for chemical measurement of NO_2 concentrations. When the mylar reservoir appeared to be empty, the face mask was disconnected from the Wright spirometer and the animal was allowed to breathe room air. Pulmonary radioactivity continued to be monitored for the next 20 minutes of this wash-out period. Three or four arterial blood specimens were obtained during the experiment. This experiment was repeated once for each animal.

The experiments with ^{125}Xe were performed in an identical fashion with the exception that the concentration of xenon was not measured chemically. The ^{125}Xe was administered prior to the repeat exposure to $^{13}NO_2$ in the first series, of experiments and following the repeat exposure to $^{13}NO_2$ in the second series.

Results

Table 1 shows the radioisotopic and chemical concentrations of $^{13}NO_2$ in inspired and expired air and the per cent differences in these measurements for each primate. The samples of inspired air that were obtained within the first two minutes of the experiment contained 0.14 to 0.36 μCi /10 ml of radioactivity. Subsequent samples in three of the four experiments had at least twice as much radioactivity, 0.60 to 1.05 μCi/10 ml. More equal concentrations with less radioactivity, 0.14 and 0.13 μCi/10 ml, were recorded in one experiment. These latter values may be artifactually low as the discriminator settings were inadvertently set for ^{125}Xe The radioactivity concentrations of the expired air at two to four minutes after the onset of the experiment varied from 0.07 to 0.54 μCi/10 ml. A second sample of expired air was measured in three experiments and in each instance the concentration of radioactivity was 20 to 30% higher. Comparison of the maximum radioactivity concentrations in the samples of inspired and expired air reveals a 30 to 50 per cent decrease in the samples of expired air. The samples with maximum radioactivity were compared as these specimens were obtained later in the experimental period and they therefore contained less pre-existing non-radioactive air.

The chemical concentrations of NO_2 in the inspired air varied from 0.30 to 0.91 ppm. The concentration of NO_2 in expired air was measured in two experiments. Comparison of these values, 0.25 and 0.11 ppm, with corresponding values for inspired air, 0.54 and 0.30 ppm, reveals decreases of 54 and 63% in NO_2 concentration.

Table 2 shows the radioactivity measurements for ^{125}Xe in inspired and expired air at various times after the introduction of this gas into the mylar reservoir. Specimens of inspired air from the first minute of the experiment had less radioactivity, 3.78 and 0.55 μCi/10 ml,

than did subsequent specimens, 3.86 and 0.81 μCi/10 ml. The concentrations of radioactivity in the expired air were 3.35 and 3.67 μCi/10 ml in the first experiment and 0.65 μCi/10 ml in the second experiment. Comparison of these values shows that the expired air contained 5 and 20% less ^{125}Xe than did the inspired air.

The scintiphotos in Figure 2 illustrate the intra and extrapulmonary radioactivity patterns for $^{13}NO_2$ and ^{125}Xe. The vertical rectangles enclose the regions in which total radioactivity was measured continuously to determine the adsorption and retention of radioactive gas. The horizontal regions were used to study the intrapulmonary distribution of gas. Two factors account for the more distinct pulmonary outlines in the scintiphoto of ^{125}Xe activity as compared to $^{13}NO_2$. Firstly, the counting efficiency of the Anger camera is considerably better for the 188 KeV gamma rays of ^{125}Xe than for the 511 KeV gamma rays of ^{13}N. Secondly, the ^{13}N radioactivity was less confined to the lung as more of the $^{13}NO_2$ entered and remained within the blood and other extrapulmonary tissues.

Figure 3 compares the curves of pulmonary radioactivity following the inhalation of $^{13}NO_2$ and ^{125}Xe in primate #2. Nearly identical relationships existed in experiments with primate #3. Exposure to 0.54 or 0.91 ppm of radioactively labeled $^{13}NO_2$ resulted in increasing pulmonary radioactivity during the 9 minute exposure period and the retention of this radioactivity throughout the 21 minute post-exposure period. The maximum net activity in both experiments was 6,000 cpm. ml. In contrast the inhalation of ^{125}Xe resulted in a more rapid increase in pulmonary radioactivity, during the exposure period and a precipitous decline to negligible decline levels when the exposure was discontinued. The maximum net activity in this experiment was 5,000 cpm. ml. Figure 4 compares the distribution of $^{13}NO_2$ and 125 Xe radioactivity in transverse sections through the upper and lower regions of the lung for primate #2. The regions from which the data were obtained are shown in Figure 2. The pattern of distribution of the two radioactive gases is relatively similar for both transverse sections. The principle difference between the radioisotopic distributions is that the lower lobe transverse section contained a higher concentration of ^{125}Xe than did the upper section, whereas the opposite result occurred with $^{13}NO_2$. The pulmonary distribution of $^{13}NO_2$ was uniform without evidence of specific regional affinity.

Blood Radioactivity. Table 3 contains the radioactivity measurements for the arterial blood specimens. The blood concentrations of ^{13}N increased to maximum values of 0.30 to 0.46 μCi/2/5 ml during the early post-exposure period in three of the four experiments. Considerable radioactivity (0.25 to 0.34 μCi/2.5 ml of blood) was still present in specimens that were obtained at the end of the post-exposure period. This pattern of result was found in the fourth experiment but due to the less accurate discriminator settings the apparent radioactivity values were much lower (Peak concentration corresponding to 0.063 μCi/2.5 ml blood.)

The blood concentrations of ^{125}Xe were maximal (0.76 μCi/2.5 ml--1st experiment; 0.055 μCi/2.5 ml--2nd experiment) near the end of the exposure period. In contrast to ^{13}N blood radioactivity, ^{125}Xe radioactivity declined rapidly in the immediate post-exposure period. Figure 5 illustrates the temporal relationships for blood and pulmonary radioactivity for the two radioisotopically labeled gases. The similarity in pattern between the blood and pulmonary concentration for each gas is apparent.

Discussion

A complete description of the complex reaction sequences occurring within the target are beyond the scope of this work. However, consideration of the kinetic data reported for reaction of nitrogen atoms generated by conventional, radiolytic, or nuclear methods, indicates that successful production of $^{13}NO_2$ in O_2-N_2 systems probably depends on adequate control of competitive reactions (1) and (2), (12-14).

(1) $^{13}N + N_2 \xrightarrow{k_1} {}^{13}N\text{-}N + N$ $\quad k_1\ (298^oK) = 3.2 \times 10^{10}$ liter mole $^{-1}$ sec $^{-1}$ for N_2

(2) $^{13}N + O_3 \xrightarrow{k_2} {}^{13}NO + O_2$ $\quad k_2\ (298^oK) = 3.4 \times 10^{8}$ liter mole $^{-1}$ sec $^{-1}$

Although a spectrum of translationally and electronically excited ionic, atomic,, and molecular species are present under the conditions of irradiation, the available evidence suggests that a k_1/k_2 value of $\sim 10^2$ is reasonable. The steady-state concentration of ozone in the target must be maintained at a level 2-3 orders of magnitude greater than any N_2 impurities in the target gas if $^{13}NO_2$ production is to be efficient, since reaction (2) determines the extent of Reaction 3.[15]

(3) $^{13}NO + O_3 \xrightarrow{k_3} {}^{13}NO_2 + O_2$ $\quad k_3\ (298^oK) = 10^7$ liter mole $^{-1}$ sec $^{-1}$

The dynamic measurements were made at a constant molecular transport rate (N_t/ unit time) of 6 x 10^{21} molecules/min (250 cc/min, 1 atm, 25°C) as this rate yielded acceptable values for production, decay in transit, and wall loss functions. Determination of the integrated radiation dose and theoretical isotope production values required computation of the average residence time (t_r) in the target (86cc) and effluent line (110cc). This may be obtained by division of the steady-state number of molecules (N_s) in a given volume segment (V_s) by the molecular transfer rate; however, the value of N_s can be derived directly from PV relationships as represented by the following expression:

$$\frac{V_s N_A}{R\ N_t/\text{min}} \left(\frac{P}{T}\right) = t_r\ (\text{min}) \qquad N_A = 6.02 \times 10^{23} \text{molecules}$$

Under the conditions imposed, the first term in this expression is a constant, and t_r varies linearly with pressure for isothermal operation. Because the molecular density, N_s /V, varies as a function of P/T, the proton energy attenuation coefficient also varies with t_r. The dependence of radiolytic ozone production on dose alone was measured under isobaric and isothermal conditions by varying the beam current. Ozone measurements at levels above 300 ppm were made on-line, using an ultraviolet spectrophotometer fitted with a 1 cm path length flow cell. Measurements in the range of 0.1 ppm and below were made with a Mast Development Co. ozone meter (Model 724-2).

The measurement of unlabeled NO_2 in the irradiated effluent gas and in NO_2 "spiked" purge gas, which were introduced for the purpose of determining losses via wall reactions, was done by the Saltzman colorimetric method.(2)

Fractional loss of NO_2 in the system, determined by the introduction of purge gas containing 10 ppm NO_2, may be qualitatively represented over a 120 hr period as 0.25 (1-exp[-1.38t]), where t is the residence time of the gas in the target (hrs.) This corresponded to an initial loss of ≃ 0.06 ppm/min. Chromatographic determinations were made with a Porapak Q column, 2.5 m long by 2.5 mm ID, connected in series with a similar Porapak R column, as reported by Wilhite and Hollis.(13) The columns were coupled with electron capture and radioactivity detectors in series. Although Trowell (4) reports that NO_2 converts to NO in these columns, we have found that the $^{13}NO_2$ fraction corresponds with that determined cryogenically if 0.25 cc-atm of NO_2 carrier is admixed with the radioactive gases prior to injection into columns which were preconditioned by multiple injections of NO_2. Analysis of the target gas before and after irradiation by high resolution mass spectrometry revealed no hydrocarbon impurities or radiolytically produced derivatives.

The reaction of radiolytic or sufficiently thermalized nuclear recoil N atoms with NO and NO_2 to produce ^{13}N-N or N_2 is also very fast and proceeds with a rate constant in the range of 1-2 x 10^{10} liter $mole^{-1}$ sec^{-1}, which is comparable to k_1; the similar direct reaction with O_2 to form NO has an appreciable activation energy and $k(300^oK)$ = 5.6 x 10^4 liter $mole^{-1}$ sec^{-1}. (14) The macroscopic concentration of NO_x compounds never exceeds the initial concentration of the N_2 impurity, since these compounds are formed via in situ radiolysis of N_2. Indeed, the sum of the steady-state N_2, NO, and NO_2 concentrations is a constant equal to the initial N_2 concentration, and by coincidence of similar reactivity to N atoms, leaves the concentration requirements for steady-state ozone unaffected.

The results from the direct measurements of ozone concentration by UV absorption at 2650 A (ε = 2540 M^{-1} cm^{-1}) over a 2-11 atm pressure range are shown in Figure 6. A fractional decrease in$[O_3]$ of 0.36 is observed as pressure and radiation dose are increased by factors of 5 and 3.5, respectively. The effects of a similar increase in dose were examined at fixed pressure of 10 atm by raising the beam current to 3.5 μA. These conditions produced a fractional decrease in $[O_3]$ of 0.31 and a measured value of ≃ 2400 ppm. Comparable measurements at 11.6 atm and 5μA indicated ≃ 2000 ppm O_3 in the effluent stream. The decreasing yields of ozone correlated primarily with increasing dose rather than pressure dependent molecular density of "stopping-power" effects. The experimental $G(O_3)$ values, which range from 3.4 downward to 0.4 as the dose is increased, are lower limits because of heterogenously catalyzed ozone decomposition at metal surfaces in the target and transfer line [16]. This process is expected to be accelerated at those internal surfaces which are heated by the proton beam. These considerations, together with reports [12] that $G(O_3)$ values for α-particle radiolysis in oxygen flow systems range from 3.9 to 7.8, is evidence that ozone concentrations in the target are at least three times those measured in the effluent. Hence, the postulated necessary condition of $[O_3]/[N_2] > 10^2$ for successful competition of reactions (2) and (3) is met if the N_2 content of the target has is 20 ppm or less.

Extraction of $^{13}NO_2$ formed is complicated by Reaction 4 [15-17].

(4) $^{13}NO_2 + O_3 \xrightarrow{k_4} {}^{13}NO_3 + O_2$ $\quad k_4\ (298^oK) = 2.6 \times 10^4$ liter $mole^{-1}$ sec^{-1}

This is rapidly followed by Reactions 5 and possibly 6.

(5) $^{13}NO_3 + NO_2 \longrightarrow {}^{13}N_2O_5$

(6) $^{13}N_2O_5 + H_2O \longrightarrow H^{13}NO_3 + HNO_3$

Although the rate determining Reaction 4 is relatively slow, the

formation of N_2O_5 proceeds with a half-life < 0.1 sec when $[O_3]$ > 2700 ppm (18).

The $^{13}N_2O_5$ and related product fraction is lost quantitatively on the walls, and the solution to the practical problem of $^{13}NO_2$ recovery consists of adjusting the target conditions to maximize Reaction 3 and minimize Reaction 5. Heating of the target walls and a portion of the effluent line depletes the ozone concentration and thermally decomposes N_2O_5 to NO_2 and O_2. Figure 7 shows the relative increase of collectible $^{13}NO_2$ activity in the cold trap as a function of increasing target wall temperature when the heated loop is maintained at 225°C. Operation of the target at 400°, allows approximately one order of magnitude more $^{13}NO_2$ to be collected than is possible at ambient temperature.

The volatile ^{13}N activity is distributed among $^{13}N_2$, $^{13}N_2O$, and $^{13}NO_2$ in the ratio of 8:1:3.5, respectively. This was observed for both static, ambient temperature, and dynamic, elevated temperature irradiations to total doses equivalent to 4-5 eV/molecule. Continued loss of gaseous $^{13}NO_2$ via Reaction 4 at the end of the static run was quenched by addition of a 100-fold excess of NO_2 as compared to O_3. Although the immediate introduction of the high temperature target effluent into a heated transfer line loop is also for the purpose of blocking Reaction 4, the coincidence of product distributions may be fortuitous. Removal of the heated loop results in loss of the $^{13}NO_2$ fraction, whereas ambient operation of the target results in uniform depletion of all yields.

The experiments in which Rhesus Monkeys were exposed for several minutes to 0.3 to 0.9 ppm of radioactively labeled $^{13}NO_2$ demonstrated that the pollutant was absorbed and retained following cessation of exposure. The reactivity of nitrogen dioxide with pulmonary tissues can be assessed from the radioactivity data of the lungs and of the entering and exiting gases. Since the two series of experiments yielded similar results, only data from primate #2 will be discussed. The slopes of the initial and precessation periods of $^{13}NO_2$ exposure were initial 900,900 precessation 900,900 Fig 3A. These values indicate a uniform pulmonary rate of absorption throughout the seven to nine minute exposure period. Further study of the washout phase of this curve indicates that expulsion of the pollutant by pulmonary washout mechanisms was negligible. Hence the overall effect of introducing nitrogen dioxide into the lungs is a firm binding of a portion of the inspired gas by pulmonary tissues, a subsequent build-up of nitrogen dioxide or chemically derived compounds, and the retention of the pollutant or its products following cessation of exposure.

The radioactive data obtained with the slightly soluble but otherwise inert ^{125}Xe shows what would have occurred if the pollutant had not reacted the vigorously with pulmonary tissues. Xenon- 125 radioactivity within the lung increased at a rapid rate during the early exposure period (slope = 1500), but because the noble gas is non-reactive, equilibrium was soon approached due to expiration of the radioactive gas and the slope diminished to 222. The magnitude of these removal mechanisms is attested to by the rapid decline in pulmonary radioactivity in the early washout period.

The extent of absorption of $^{13}NO_2$ by the lung can be inferred by comparing the radioactivity of the inspired and expired air. According to these data from 30 to 50 percent of the inspired nitrogen dioxide remained within the lungs. It is noteworthy that there was a 5% decline in the concentration of expired ^{125}Xe in one experiment and an 18 percent decline in the second experiment in which only a single non-equilibrium value of expiratory ^{125}Xe was available.

Comparisons of the pulmonary distribution of $^{13}NO_2$ and ^{125}Xe indicate that the absorption of the pollutant slightly altered its distribution. That is, less of the $^{13}NO_2$ reached the lower lungs than would be expected if the normal gas distribution patterns had prevailed. The most likely explanation for this occurrence is that a significant quantity of $^{13}NO_2$ was absorbed in the proximal pulmonary regions thereby diminishing the amount of gas reaching the more distal pulmonary regions.

The measurements of arterial blood radioactivity indicate that $^{13}NO_2$ or a chemical derivative readily passes the alveolar-blood barrier. The concentration of this compound within the blood increases in parallel with the intrapulmonary concentration of the pollutant. Inspired nitrogen dioxide is therefore capable of causing biological effects of intrapulmonary sites. The available information is insufficient to evaluate this newly discovered potential for injury.

The finding that absorbed $^{13}NO_2$ is not removed by pulmonary wash-out mechanisms is of particular importance. Because absorbed $^{13}NO_2$ is retained in entirety by the lung, continuous exposure to the pollutant results in the accumulation of $^{13}NO_2$ or chemically derivatives at the site of reaction. This increase in concentration imposes an additional risk to tissues that are subjected to the pollutant. It seems likely that as the intensity of interaction increases, the propensity for biological injury becomes proportionately greater. This physiological relationship may explain the lack of adverse consequences following brief exposures to nitrogen dioxide whereas more prolonged exposures to the same concentrations of nitrogen dioxide can cause appreciable injury.

References

1. Stokinger, H.E. and Coffin, D.L. 1968. Biological effects of air pollutants. In Air Pollution. A.C. Stern, Editor. Academic Press. Inc. New York. 2nd. Edition. 445-546.

2. Speizer, F.E. and Frank, N.R. 1966. The uptake and release of SO_2 by the human nose. Arch. Environ. Hlth. 12:725-728.

3. Frank, N.R., Yoder, R.E., Yokoyama, E. and Speizer, F.E.1967. The diffusion of $^{35}SO_2$ from tissue fluids into the lungs following exposure of dogs to $^{35}SO_2$. Health Physics. 13:31-38.

4. Frank, N.R. Studies on the effects of acute exposure to sulphur dioxide in human subjects. 1964. Proc. Roy. Soc. Med. 57:1029-1033.

5. Koch-Weser J. Common poisons. In Harrison's Principles of Internal Medicine. McGraw-Hill Book Company. New York. 6th. Edition. Pp. 652-654.

6. Von Nieding, G., Wagner, H., Krekeler, H., Smidt, U. and Muysers, K. Absorption of NO_2 in low concentrations in the respiratory tract and its acute effects on lung function and circulation Second International Clean Air Congress of the International Union of Air Pollution Prevention Associations. Dec. 6-11, 1970. Washington, D.C.

7. Yokoyama, E. 1968. Uptake of SO_2 and NO_2 by the isolated upper airways. Bull Inst. Pub. Hlth. 17:302-306.

8. Ichioka, M. 1972. Model experiments in the absorbability of the airway mucous membrane of SO_2 and NO_2 gas. Bull Tokyo Med. Dent. Univ. 10:361-375.

9. Parks, N.S., Peek, N.F., and Goldstein, E. Int. J. Appl. Radiat. Isotop. In press.

10. Hines, H.D., Peek, N.F., DeNardo, G.L. and Jansholt, A.L. 1975. Production and characteristics of ^{125}Xe: A new noble gas for in vivo studies. N. Nucl. Med. 16:143-147.

11. Saltzman, B.E.1965. In Selected methods for the measurement of air pollutants. Environmental Health Series, Public Health Service Pub. No. 999-AP-11, U.S. Government Printing Office. Washington, D.C. D1-D5.

12. Anderson, A.R. 1968. Inorganic Cases. In Fundamental Processes in Radiation Chemistry. P. Ausloos. Editor. John Wiley and Sons. New York. Pp. 311.

References Cont'd.

13. Welch, M.J. 1968. Production of active molecular nitrogen by the reaction of recoil nitrogen-13. Chem. Comm. No. 21. 3:1354.

14. Brocklehurst, B. and Jennings, K.R. 1967. Reaction of nitrogen atoms in the gas phase. In Progress in Reaction Kinetics.E.Porter, Editor. Pergamon Press. London.

15. Ghormley, J.A., Ellsworth, R.L. and Hochanadel, C.J. 1973. Reaction of exceted oxygen atoms with nitrous oxide. Rate constants for reaction of ozone with nitric oxide and with nitrogen oxide. J. Phys. Chem. 77:1341.

16. Denson, Sidney W., Axworthy, Arthur E. Jr. 1959. Implications of data on the gas phase decomposition of ozone. Advances in Chemistry Series. (Ozonic Chem. and Tech.) 21:1959.

17. Wu, C.H., Morris, E.D. and Niki, H. 1973. The reaction of Nitrogen oxide with ozone. J. Phys. Chem. 77:2507.

18. Saltzman, B.E. 1973. Analytical methodologies for nitrogen oxides in perspective. Proceedings of the Conference on Health Effects of Air Pollutants. Assembly of Life Sciences of the National Academy of Sciences., National Research Council Serial No. 93-15 U.S. Government Printing Office. Stock No. 5270-02105. Pp. 317-344.

List of Publications

1. Parks, N.J., Peek, N.F., Goldstein, E. The synthesis of ^{13}N labeled atmospheric gases via proton irradiation of a high pressure oxygen target. Int. J. Appl. Radiat. Isot. In press.

2. Goldstein, E., Peek, N.F., Parks, N.J., Hines, H.H., Steffey, E.P., and Tarkington, B. Fate and distribution of inhaled nitrogen dioxide in the non-human primate. Abstract, accepted for presentation at the XXIII conference of the International Union Against Tuberculosis. Mexico City, September 22-26, 1975.

3. A manuscript of the above presentation is in preparation.

Glossary

ppm	parts per million
ev	electron-volt
Mev	Million electro volts
mb	milli barn
μA	micro amp
μCi	microcuries
mCi	millicuries

Appendix

Figure 8 is a schematic of the experimental system. The target is a stainless steel cylinder (dimensions 27 mm I.D. by 150mm length) with a 0.058mm thick stainless steel window welded to a removable flange. Water cooling is provided at the entrance collimator and beam stop ends. Temperatures between ambient and 475°C are maintained by a remotely operated electrical heating tape that is wound around the central portion of the target. A thermocouple gauge monitors the temperature. The target is electrically isolated so that the beam current can be monitored separately at the collimator and the beam stop. Thirty meter lengths of stainless steel tubing (2.2mm I.D.) connect the target to the gas handling system in the radiochemistry laboratory. Immediately down-stream of the target is a 4-meter long spiral trap enclosed in a remotely operated electrical tube furnace, allowing further temperature control of the effluent gases.

The effluent gases are separated in a cryogenic spiral trap at -45°C. The NO_2/N_2O_4 fraction ($f.p._{NO_2}$ = 9.3°C) freezes at this temperature, whereas the more volatile N_2, N_2O, and NO components remain gaseous and exit from the collection system. The radioactivity in the cryogenic trap and the tubing downstream is monitored by two collimated NaI(Tℓ) detectors in conjunction with two spectrometer systems that drive a dual channel chart recorder. The detectors are calibrated with a standard ^{22}Na positron source placed in a comparable geometry.

Gas circulation is provided by a stainless steel diaphragm pump which permits selectable displacement rates (0-700 cc/min. by micrometer adjustment) at a constant input-output pressure.

The target gas is Matheson "UHP" grade oxygen (99.99%). A gas pressure of 11.6 atm is maintained during the production runs to provide a target thickness of 250 mg/cm^2. The 15 MeV incident proton beam loses 10 MeV of energy to the target gas under these conditions, thereby allowing maximum use of the ≃ 200 mb integrated (p,α) cross-section [10]. This corresponds to a radiation dose of 6 x 10^{19} eV/sec/μA. Elevated pressures offer the advantages of (1) practical target size, (2) minimum loss of ^{13}N to the target walls by nuclear recoil following the (p,α) reaction, and (3) enhanced production of $^{13}NO_x$ compounds[1]. The lifetime of the beam foil at elevated pressures is 10-30 μA-hours for a 5-10 μA beam focused to about 3mm^2 and continuously swept within the confines of a 12.5mm diameter graphite collimator. Operation in flow-through or recirculating mode provides improved recovery of short-lived labeled compounds, additional control over radiation dose, and extended life of the beam foil. All components of the system were especially prepared for high pressure oxygen service in order to obviate the significant potential hazard of oxygen-oil explosion.

Figure 1

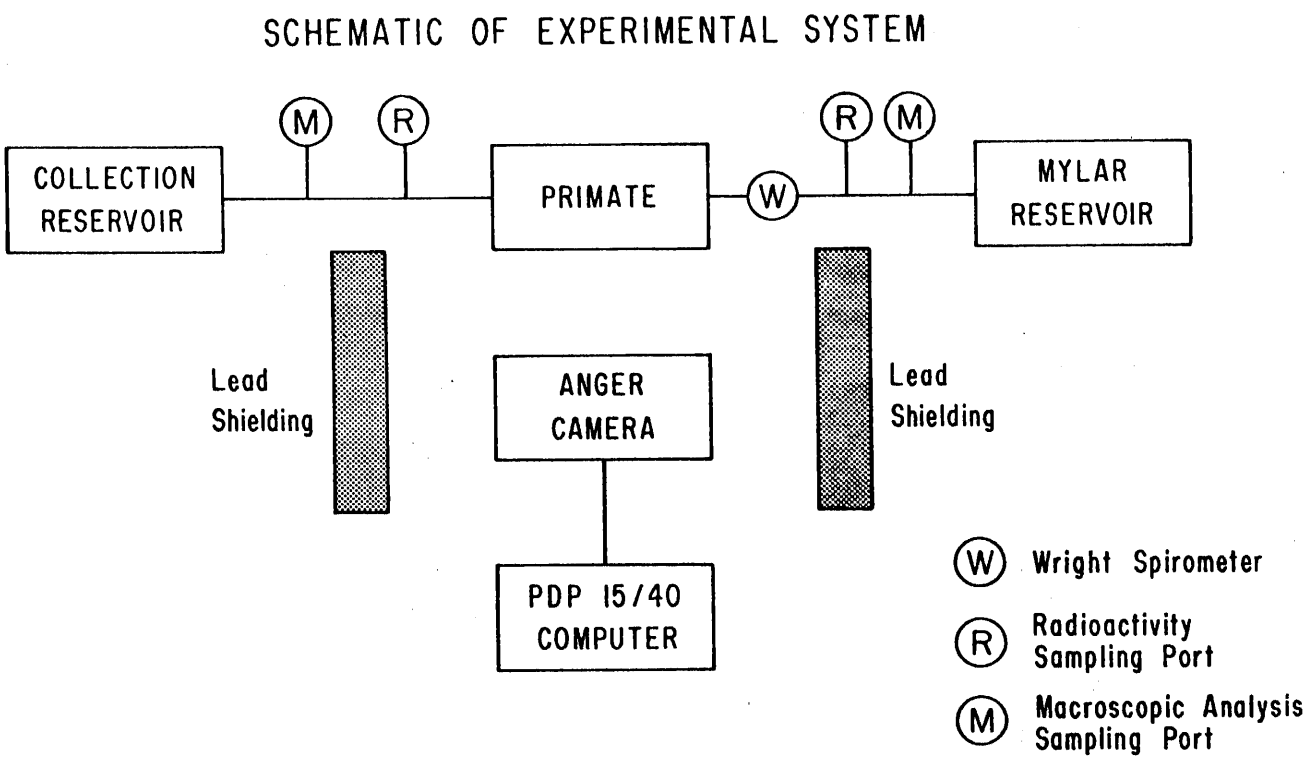
SCHEMATIC OF EXPERIMENTAL SYSTEM
M
R
R
M
COLLECTION RESERVOIR
PRIMATE
W
MYLAR RESERVOIR
Lead Shielding
ANGER CAMERA
Lead Shielding
PDP 15/40 COMPUTER
W Wright Spirometer
R Radioactivity Sampling Port
M Macroscopic Analysis Sampling Port

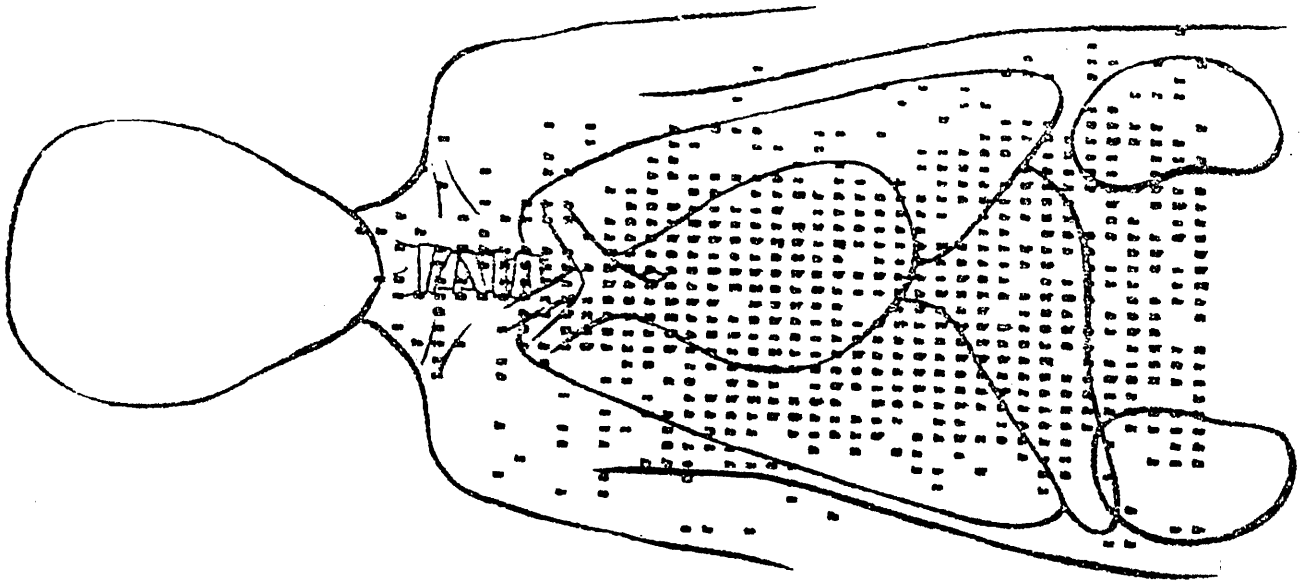

b

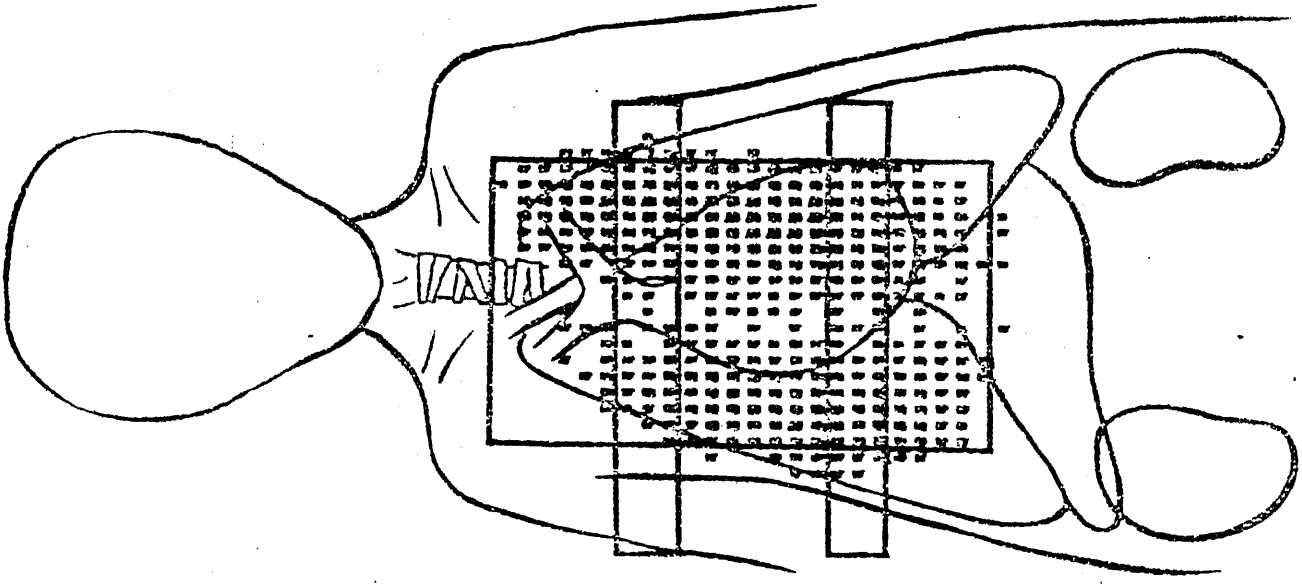

a

Figure 2

Figure 3

TEMPORAL COMPARISON OF PULMONARY
$^{13}NO_2$ AND ^{125}Xe (ANIMAL NO. 2)

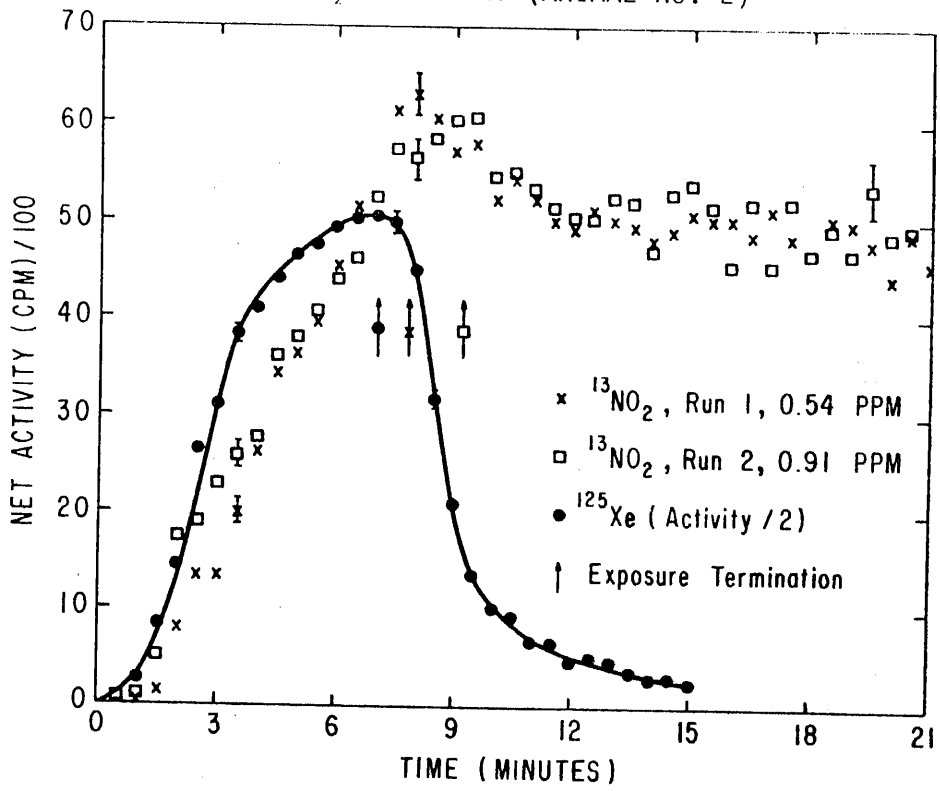

TEMPORAL COMPARISON OF PULMONARY
$^{13}NO_2$ AND ^{125}Xe (ANIMAL NO. 3)

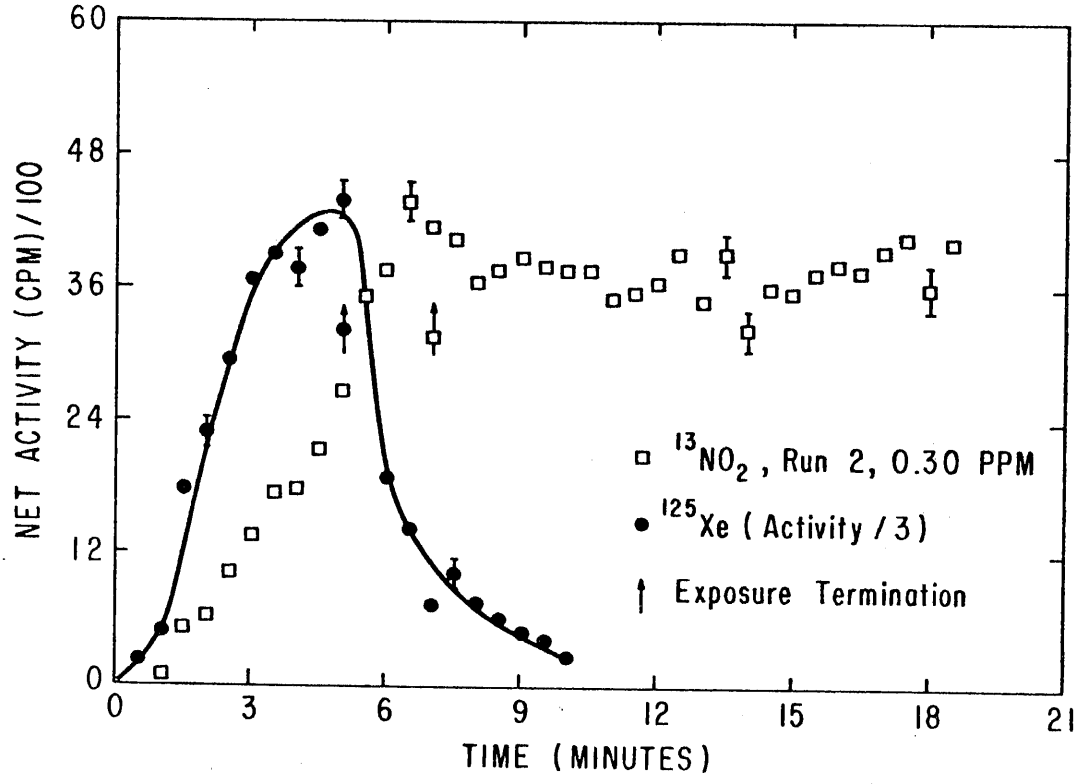

Figure 4

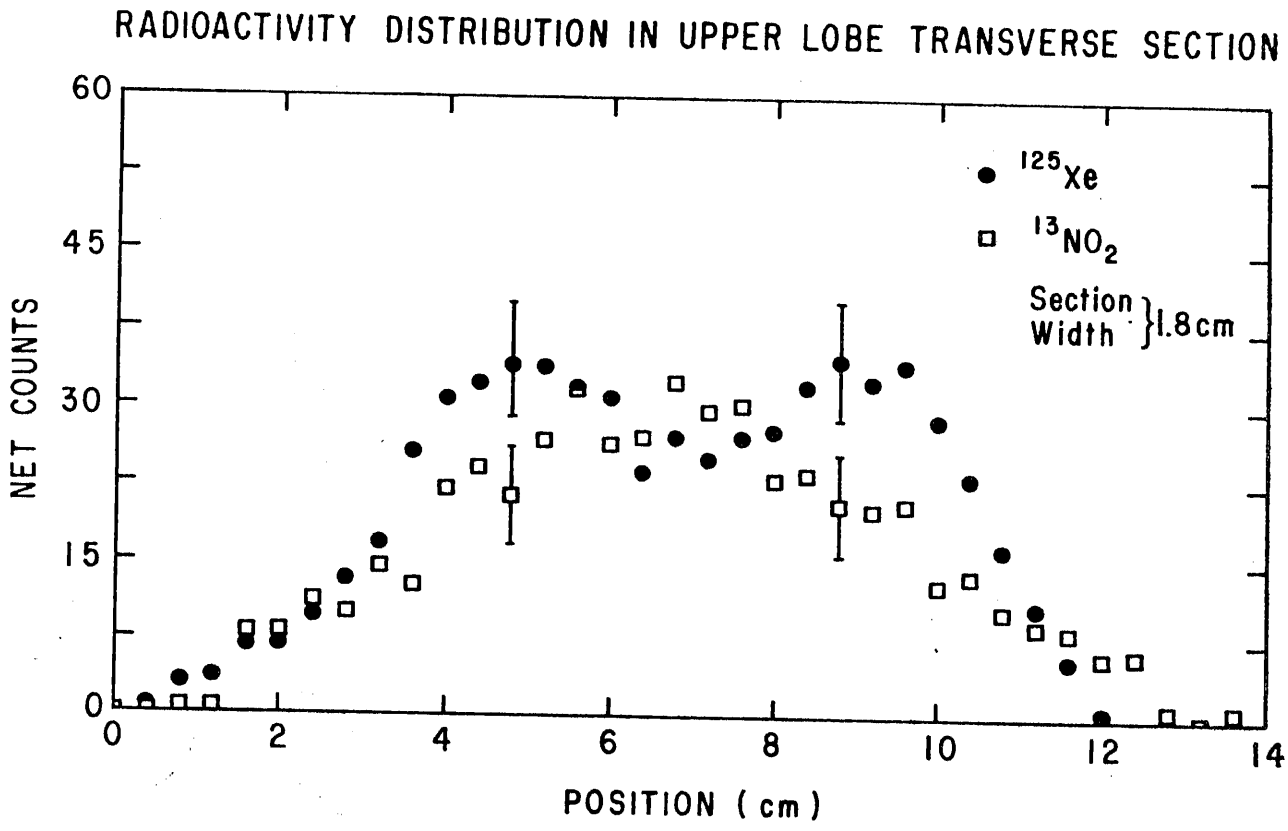
RADIOACTIVITY DISTRIBUTION IN UPPER LOBE TRANSVERSE SECTION
NET COUNTS
POSITION (cm)
^{125}Xe
$^{13}NO_2$
Section Width 1.8cm
0
15
30
45
60
0
2
4
6
8
10
12
14

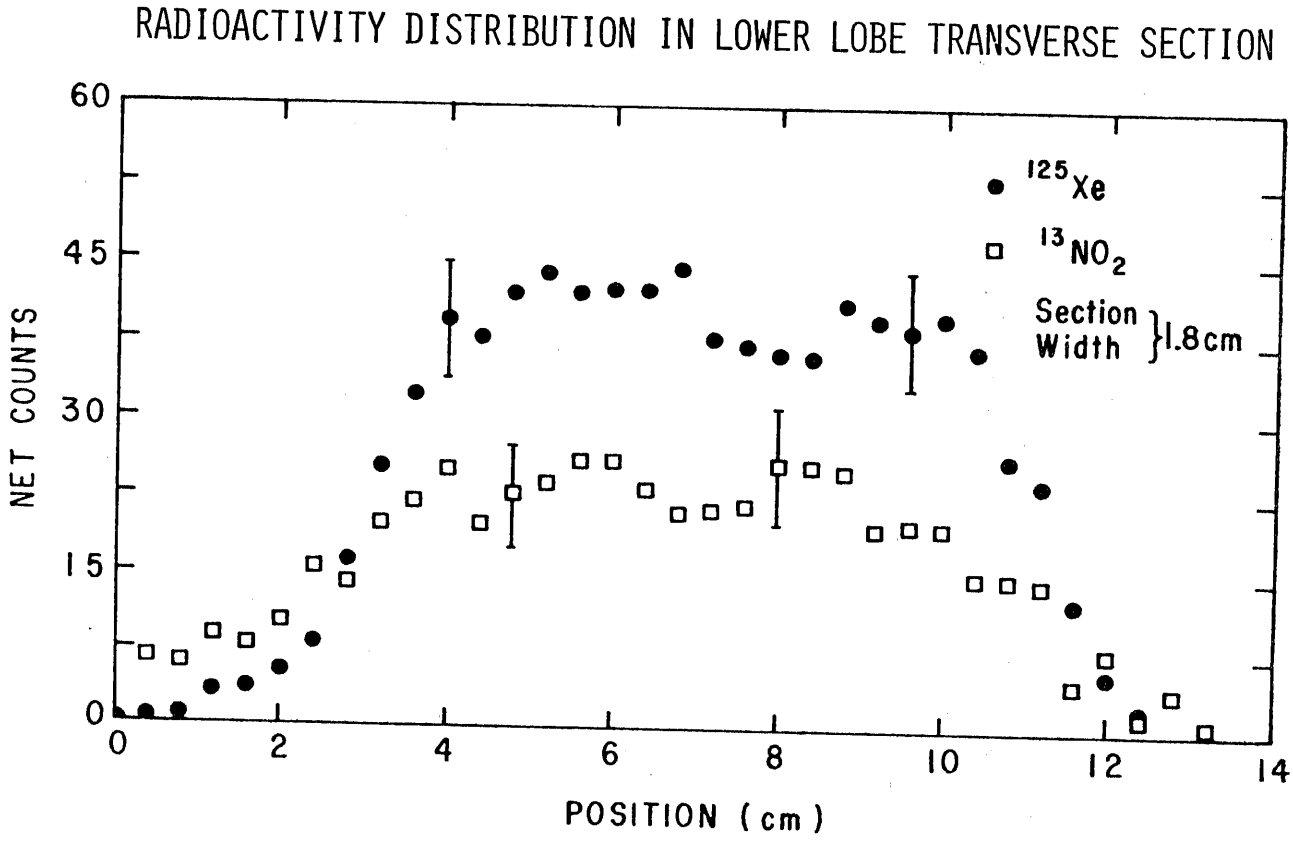
RADIOACTIVITY DISTRIBUTION IN LOWER LOBE TRANSVERSE SECTION
NET COUNTS
POSITION (cm)
^{125}Xe
$^{13}NO_2$
Section Width 1.8cm
0
15
30
45
60
0
2
4
6
8
10
12
14

Figure 5

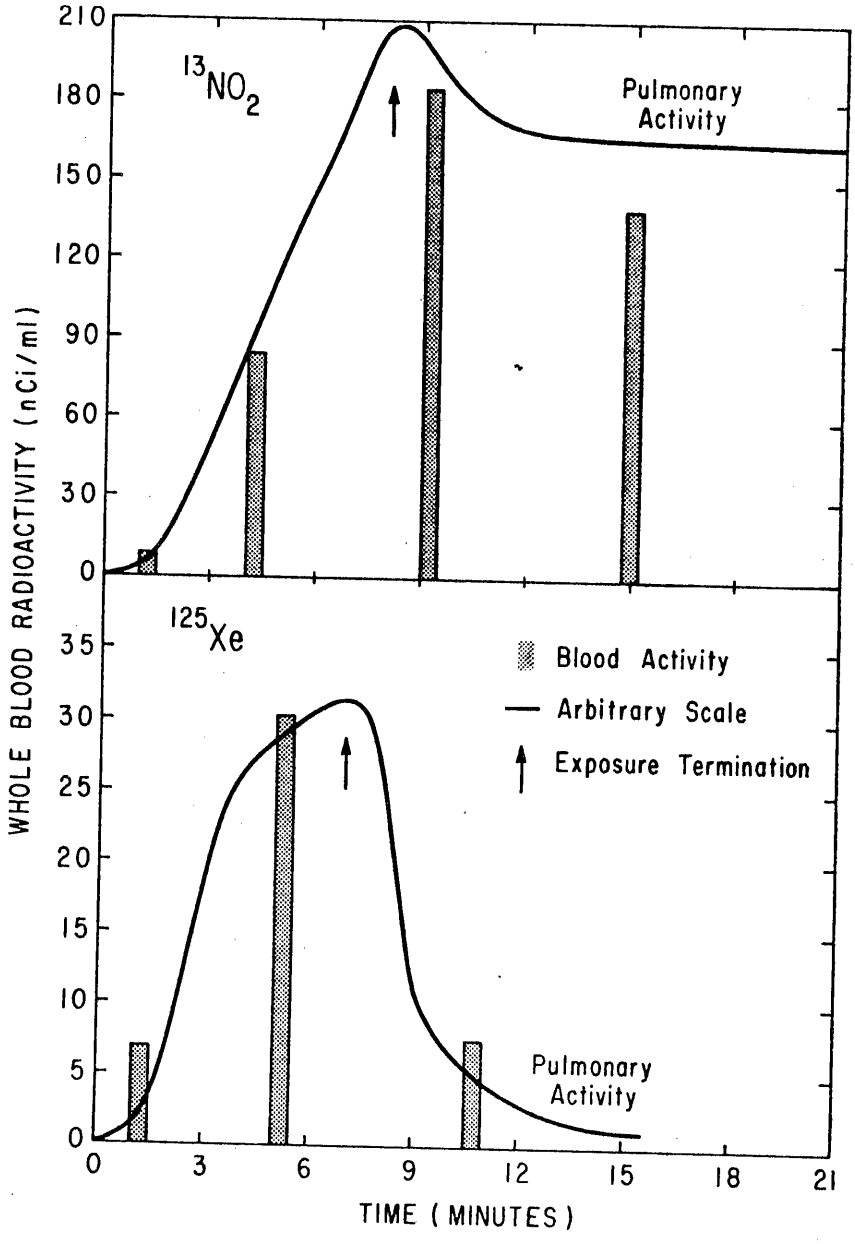
$^{13}NO_2$
Pulmonary Activity
^{125}Xe
Blood Activity
Arbitrary Scale
Exposure Termination
Pulmonary Activity
WHOLE BLOOD RADIOACTIVITY (nCi/ml)
TIME (MINUTES)
0
30
60
90
120
150
180
210
0
5
10
15
20
25
30
35
0
3
6
9
12
15
18
21

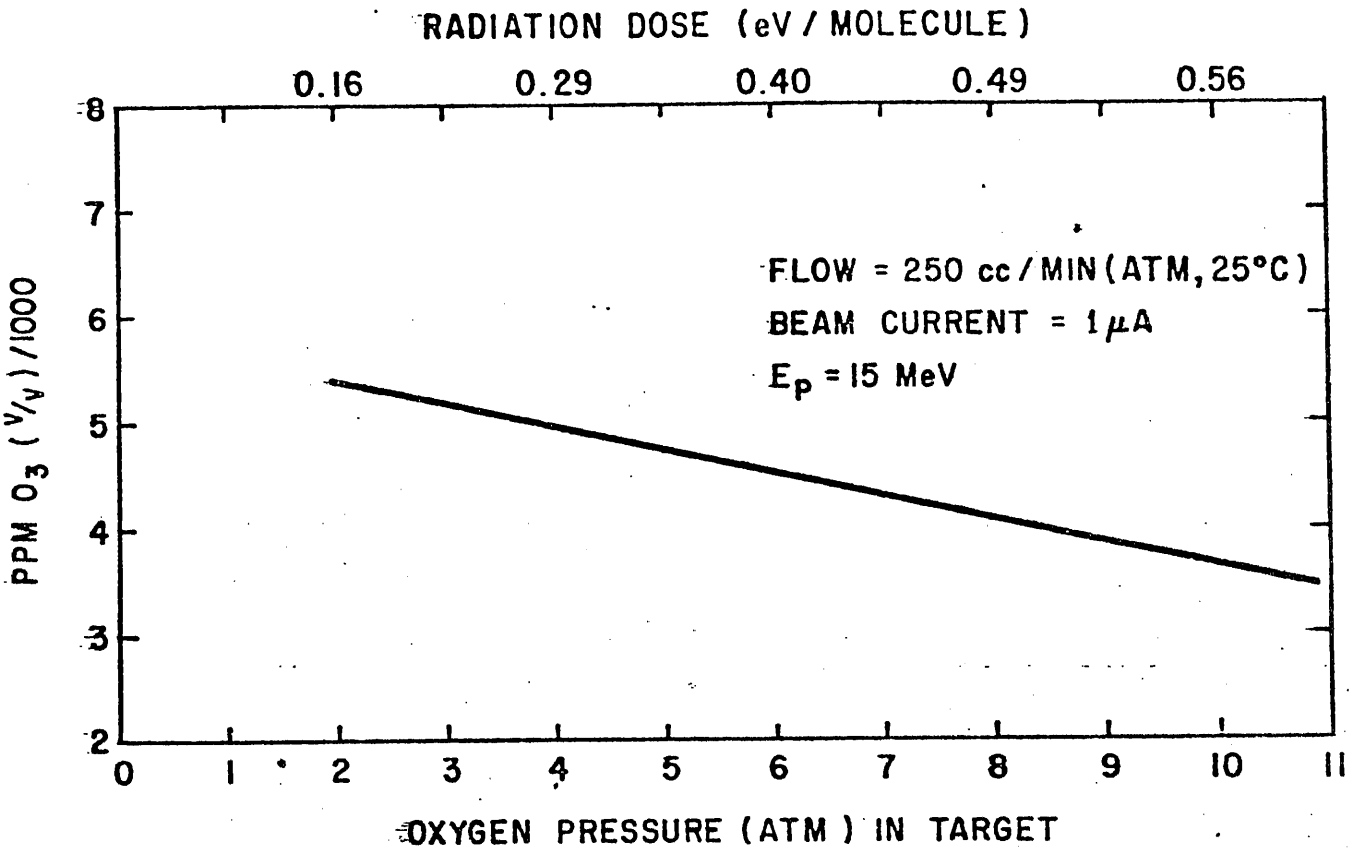

Figure 6. Relationship of ozone concentration to oxygen pressure in the target system.

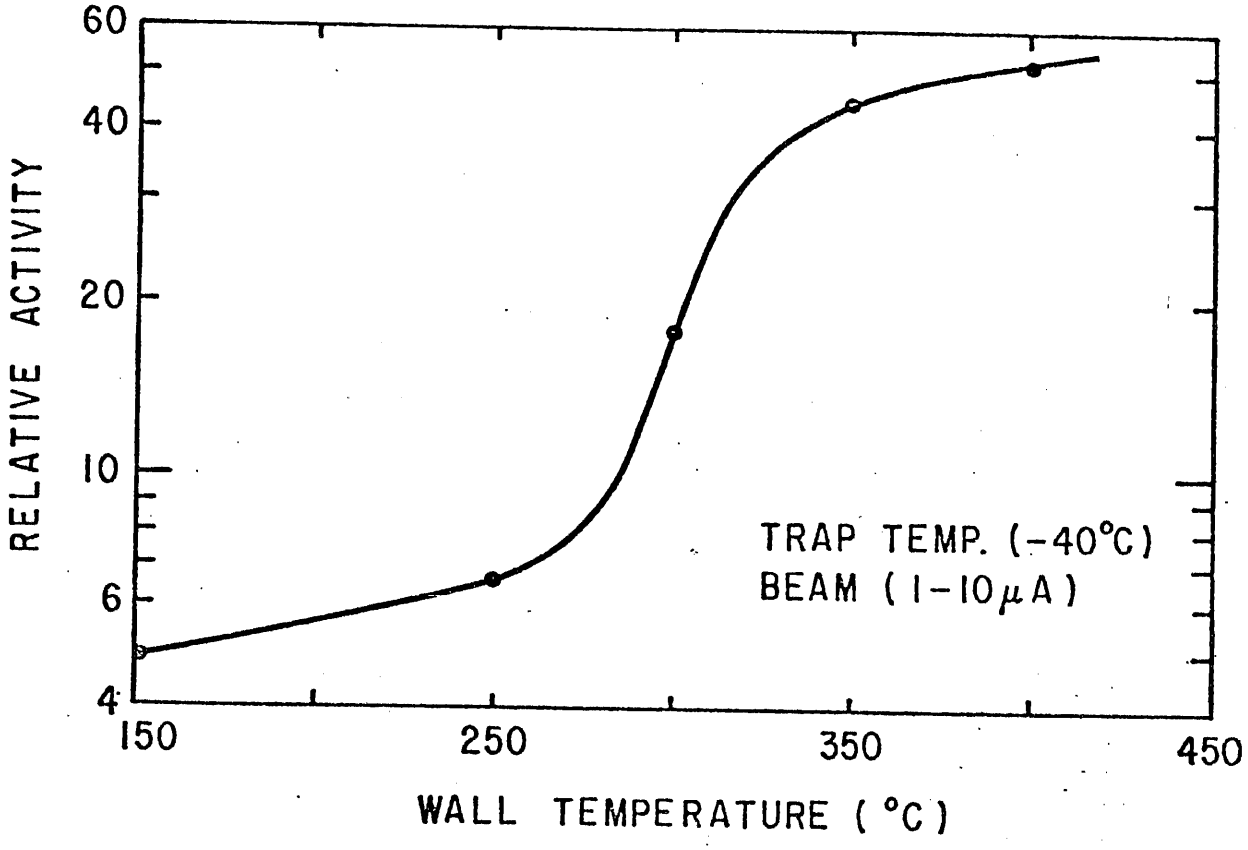

Figure 7. Increases in reactive ^{13}N radioactivity as a function of temperature of the target wall.

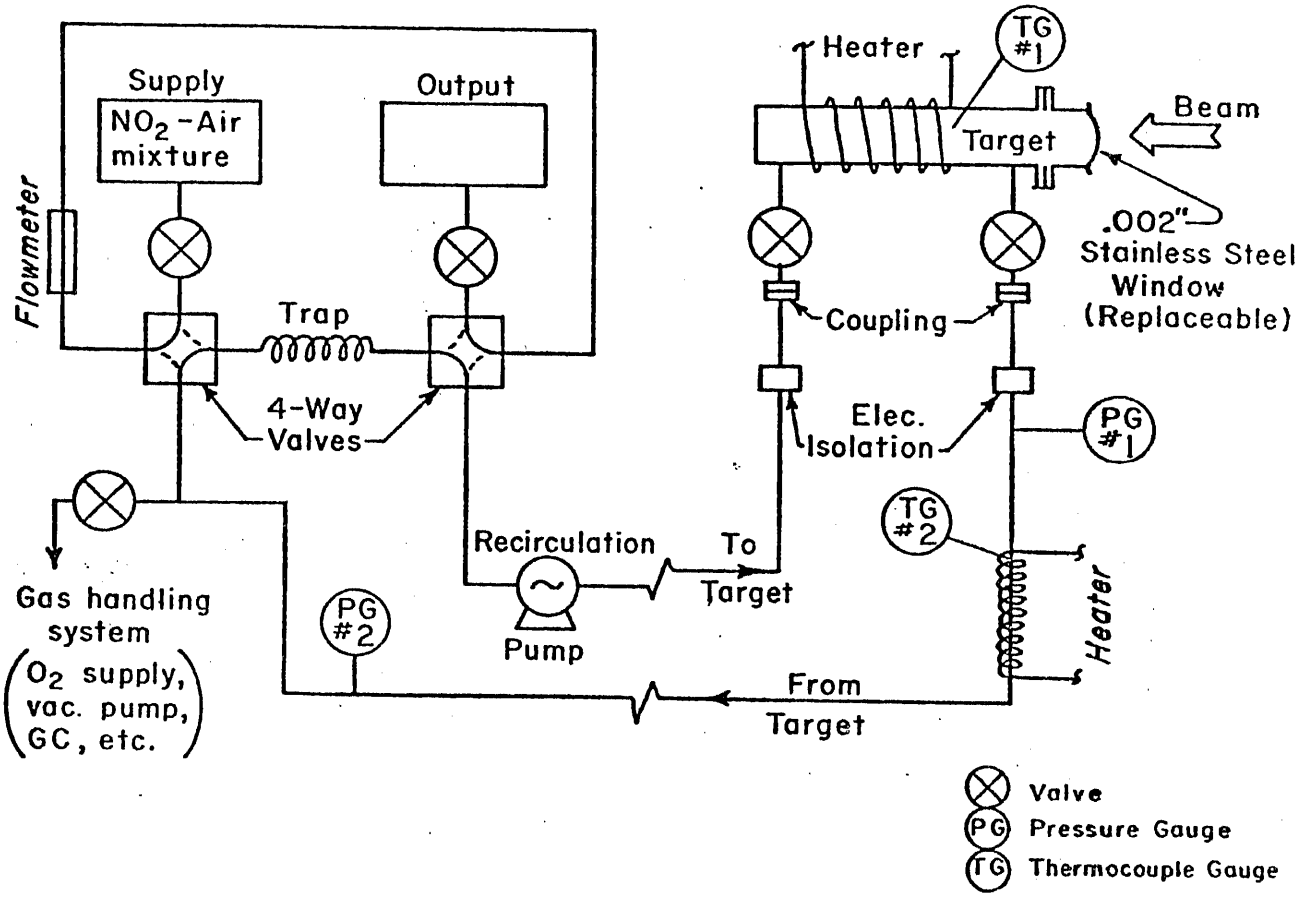

Figure 8. Schematic diagram of the experimental system used to synthesize and collect radioactive nitrogen dioxide ($^{13}NO_2$).

Table 1. Concentrations of $^{13}NO_2$ in inspired and expired air at various times after onset of exposure.

Experimental animal	Run No	Time Seconds	Radioactivity (1) Inspired	Radioactivity (1) Expired	$^{13}NO_2$ (2) Retention	Chemical Concentration (3) Inspired	Chemical Concentration (3) Expired	$[NO_2]$ Retention
2	1	83	0.36		%			%
		201		0.54				
		272	1.05		31	0.54	0.25	54
		392		0.72				
	2	47	0.28					
		198		0.37				
		283	0.65		34	0.91	---	---
		450	0.65					
		500		0.43				
3	1	90	0.14					
		130		0.07	45	0.48	---	---
		205	0.13					
	2	120	0.28					
		225		0.22	50	0.03	0.11	63
		395	0.60					
		435		0.30				

(1) µCi/10 ml
(2) Based on maximum radioactivity values for inspired and expired air.
(3) ppm

TABLE 2. Xenon-125 radioactivity in inspired and expired air at various times after onset of exposure

Experimental Animal	Time (seconds)	Radioactivity Inspired μCi/10 cc	Radioactivity Expired μCi/10 cc
2	33	3.78	
	200		3.38
	295	3.86	
	375		3.67
3	45	0.55	
	128		0.65
	210	0.81	

Table 3. Radioactivity of Arterial Blood of Non-human primates at various times after inspiration of $^{13}NO_2$ and ^{125}Xe.

Expt. 2	Time (Sec)	Activity μCi/2.5 ml	Washout (Sec)
	70	0.018 ± .004	
$^{13}NO_2$	246	0.21 ± .04	463
Run 1	733	0.46 ± .09	
	902	0.34 ± .07	
	95	.031 ± .006	
$^{13}NO_2$	261	0.22 ± .04	550
Run 2	637	0.41 ± .08	
	1285	0.21 ± .05	
	70	0.015 ± .003	
^{125}Xe	304	0.076 ± .015	425
	644	0.015 ± .003	
Expt. 3			
$^{13}NO_2$	105	0.012 ± .002	
Run 1	180	0.031 ± .006	300
	380	0.057 ± .001	
	600	0.063 ± .013	
$^{13}NO_2$	300	0.046 ± .009	455
Run 2	540	0.17 ± .03	
	900	0.30 ± .06	
	1080	0.32 ± .06	
^{125}Xe	100	0.013 ± .003	
	230	0.020 ± .004	350
	430	0.0055± .0011	
	675	0.0014± .0003	